Check for updates

View Article Online
View Journal

PCCP
Physical Chemistry Chemical Physics

Accepted Manuscript

This article can be cited before page numbers have been issued, to do this please use: L. Warczinski and C. Hattig, *Phys. Chem. Chem. Phys.*, 2019, DOI: 10.1039/C9CP04606B.



This is an Accepted Manuscript, which has been through the Royal Society of Chemistry peer review process and has been accepted for publication.

Accepted Manuscripts are published online shortly after acceptance, before technical editing, formatting and proof reading. Using this free service, authors can make their results available to the community, in citable form, before we publish the edited article. We will replace this Accepted Manuscript with the edited and formatted Advance Article as soon as it is available.

You can find more information about Accepted Manuscripts in the Information for Authors.

Please note that technical editing may introduce minor changes to the text and/or graphics, which may alter content. The journal's standard Terms & Conditions and the Ethical guidelines still apply. In no event shall the Royal Society of Chemistry be held responsible for any errors or omissions in this Accepted Manuscript or any consequences arising from the use of any information it contains.

ROYAL SOCIETY OF CHEMISTRY

rsc.li/pccp

View Article Online
DOI: 10.1039/C9CP04606B

PCCP

ARTICLE TYPE

Cite this: DOI: 10.1039/xxxxxxxxxx

Quantum chemical study of hydrogen adsorption on carbon-supported palladium clusters†

Lisa Warczinski,*[a] and Christof Hättig[a]

Received Date
Accepted Date

DOI: 10.1039/xxxxxxxxxx

www.rsc.org/journalname

A key step for achieving better insight into catalytic hydrogenations is to understand in detail the process of hydrogen adsorption on the catalyst. The present article focuses on hydrogen adsorption on carbon-supported palladium clusters, which are nowadays one of the most common catalysts in industrial applications. Density functional theory is applied to study Pd_6 and Pd_{21} clusters to reveal the influence of the carbon support material on the properties of the catalyst as well as on the mechanisms and energetics of the hydrogen adsorption. In general, a stepwise hydrogen adsorption process is observed consisting of molecular adsorption followed by a dissociative chemisorption. The carbon support material does not noticeably affect the reaction mechanisms, but has a large influence on energy barriers and preferential adsorption sites. Our comparison of Pd_6 and Pd_{21} systems reveals that small clusters, such as Pd_6, are able to model some but not all important properties of palladium nanoparticles and, therefore, it is essential to also study larger cluster sizes.

1 Introduction

Hydrogenation is one of the industrial catalytic processes with the longest history and is among the most important processes in petrochemical and fine chemicals industry.[1–4] For instance, hydrogenations are used to convert chloronitrobenzenes to chloroanilines, which are essential organic feedstocks,[5] and are part of the biomass conversion process of lignin to phenol and phenol derivatives[6]. The most common catalysts in hydrogenation reactions are metal-nanoparticles, often palladium, carried by a high-surface-area support material.[7] In early industrial applications oxide materials were the support material of choice. Over the years porous oxide supports have been replaced by novel 2D carbon support materials with high surface areas, as these are resistant to both acid and basic media and facilitate the recovery of the metal. Another advantage of these carbon materials is that their surface properties can be fine-tuned with great precision, e.g. by nitrogen or oxygen doping.[8] Even though the first industrially applied catalytic hydrogenation processes date back to more than a century ago, there are still numerous challenges in industrial catalytic hydrogenation and a detailed understanding of hydrogenation reactions, especially on carbon-supported metal-nanoparticles, has not yet been achieved.[1]

A key step in hydrogenation reactions is the hydrogen adsorption on the catalyst. Hydrogen adsorption on palladium crystal surfaces and free palladium clusters has been studied intensively in experiments[9–13] as well as in theory[14–23]. However, when it comes to hydrogen adsorption on carbon-supported palladium clusters only few publications are available in the literature. Most of the existing studies focus on hydrogen storage and are restricted to single palladium atoms or small palladium clusters with up to six palladium atoms.[24–26] To get further insight into hydrogen adsorption in the context of hydrogenation reactions, it is important to take also larger cluster sizes into account, which are more realistic models of the palladium-nanoparticles that are used in experiments. Furthermore, it is important to study the whole process of hydrogen adsorption including reaction pathways on carbon-supported clusters and to compare them with the results for free palladium clusters.

The purpose of the current study is to shed light on the influence of carbon support materials on the electronic properties of palladium metal catalysts and their influence on hydrogen adsorption in the context of hydrogenation reactions. To study the complex interplay between hydrogen, the palladium-nanoparticles and the carbon support material, we performed state-of-the-art electronic structure calculations using density functional theory (DFT) with a meta-GGA functional.

As a part of a project on mesoporous carbon supported metal catalysts for sustainable hydrogenation reactions we are interested in palladium nanoparticles on mesoporous carbon. We chose as model systems the octahedral Pd_6, which lends itself to give a quick first insight, and a Pd_{21} cluster, which is the small-

[a] Lehrstuhl für Theoretische Chemie, Ruhr-Universität Bochum, 44780 Bochum, Germany. E-mail: lisa.warczinski@rub.de

† Electronic Supplementary Information (ESI) available: [details of any supplementary information available should be included here]. See DOI: 10.1039/cXCP00000x/

Published on 10 September 2019. Downloaded by Ruhr Universitat Bochum on 9/17/2019 4:04:55 PM.

Physical Chemistry Chemical Physics Accepted Manuscript

View Article Online
DOI: 10.1039/C9CP04606B

Published on 10 September 2019. Downloaded by Ruhr Universitat Bochum on 9/17/2019 4:04:55 PM.

Physical Chemistry Chemical Physics Accepted Manuscript

est cluster capable of representing the palladium nanoparticles used in experiments, because it reflects a palladium {111} facet and possesses two adjacent face centered cubic sites at its top. Mesoporous carbon is one of the several novel 2D carbon support materials, has an amorphous, partly graphitic structure and can be doped with nitrogen or oxygen containing groups[27–29]. As we plan to investigate in forthcoming studies the effect of nitrogen and oxygen doping of the mesoporous carbon on hydrogenations, which we believe is in the first place an effect taking place in the π-system of the graphitic parts, we decided to model the carbon support material by a hydrogen-terminated graphene layer.

2 Computational details

The present quantum chemical study was performed on the level of density functional theory (DFT) with the TPSS[30] functional and the def2-SVP[31] basis set, which employs the Stuttgart-Cologne effective core potentials (def2-ecp)[32] for the palladium atoms. We have chosen the meta-GGA TPSS functional, as TPSS offers a very good cost/performance ratio throughout the periodic table, also in transition metal chemistry,[33] and meta-GGA functionals have turned out to be an efficient and reliable tool to investigate surface interactions in previous studies[34,35].

All calculations were carried out using the TURBOMOLE[36] program package and include the multipole accelerated resolution of the identity (RI) approximation[37] with optimized auxiliary basis sets[38] and Grimme's D3 correction[39] for London dispersion interactions.

The most stable structures of the palladium clusters on the support material as well as the minima of the reaction pathways were determined by ground-state geometry optimizations. We determined the ground state multiplicity of each system by including in preliminary single point calculations a Fermi smearing of the occupation numbers and by analyzing later on the eigenvalues of the singlet and triplet stability matrices. For relative energies single point energies were combined with a vibrational analysis yielding the zero-point vibrational energy (ZPVE) corrections. For the largest carbon-supported palladium clusters included in this study (Pd_{21} clusters on 150 carbon atoms) full vibrational analysis for all structures would have been too time consuming. Results for Pd_6 and an exemplary calculation for Pd_{21} show, however, that the carbon support material makes only a minor contribution to the ZPVE correction to the adsorption and reaction energies. Therefore, the relative energies for carbon-supported Pd_{21} were corrected using the ZPVEs of the corresponding free clusters. The results of the vibrational analysis were also used to calculate Gibbs free reaction enthalpies and free activation enthalpies within the harmonic oscillator and rigid rotor approximation at reaction conditions of 298.15 K and 0.1 MPa. As mentioned above, vibrational analysis for the Pd_{21} clusters on 150 carbon atoms have not been performed and, thus, Gibbs free reaction enthalpies and free activation enthalpies are not available for these systems.

The chain-of-state method implemented in the woelfling module of TURBOMOLE[40] was used for determining reaction pathways and locating initial transition state structures. The transition state structures from the reaction pathways were used as start guess for a further optimization with the eigenvalue-following trust-region image minimization (TRIM)[41] algorithm and validated by intrinsic reaction coordinate (IRC)[42] calculations. For reasons of computational costs the transition states for the largest systems included in this study (Pd_{21} clusters on 150 carbon atoms) were directly taken from the reaction pathway optimization without further optimization. We expect the errors introduced by this approximation to be negligible for this system.

To simplify the comparison of reaction energies and Gibbs free reaction enthalpies, adsorption energies and dissociation energies are given with a negative sign. Energy barriers like activation barriers are characterized by a positive sign. Of course, DFT energetics provide at this level only a qualitative accuracy and results obtained with different functionals and basis sets can differ in the range of some kJ/mol per bond (some exemplary comparisons of the TPSS/def2-SVP results with the BP86[43,44] and PBE[45] functionals and with the def2-TZVP[31] basis set can be found in the supporting information†). Therefore, we have limited ourselves to the discussion of energetic trends, which turned out to be the same for different functionals and basis sets (see the incremental adsorption energies in the supporting information†), and we refrained from a comparison with experimental energies.

To investigate the details of the electronic structure we calculated electron densities and generated electron density difference plots and visualized intrinsic bond[46] orbitals (IBOs). For these we used at Pd a 1s1p1d subset of the atomic orbitals in the cc-pVTZ-PP basis[47].

3 Results and discussion

3.1 Carbon-supported palladium clusters

As a first step, model systems for the carbon-supported palladium clusters have to be set up. The palladium clusters have to be chosen such that they are not too large for electronic structure calculations, but can act as models for palladium nanoparticles, as they are used in experimental studies as well as in industrial hydrogenation reactions. The carbon surface has to be large enough to support the clusters.

In the present work the octahedral Pd_6 cluster on a carbon support with 96 carbon atoms and a Pd_{21} cluster on a carbon support with 150 carbon atoms are used as model systems. The Pd_6 cluster, whose structure is shown in Fig. 1, is relatively small and contains six palladium atoms that have all exactly the same coordination. The Pd_6 cluster lends itself to obtain a quick insight into the metal-support interactions between palladium clusters and the carbon support.

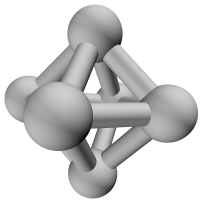


Fig. 1 Structure of the octahedral Pd_6 cluster.

To model palladium nanoparticles, as they are used in exper-

This journal is © The Royal Society of Chemistry [year]

View Article Online
DOI: 10.1039/C9CP04606B

Published on 10 September 2019. Downloaded by Ruhr Universitat Bochum on 9/17/2019 4:04:55 PM.

iments, and their adsorption interaction with H_2 molecules, we chose a Pd_{21} cluster, whose structure is shown in Fig. 2. Even though the top of the cluster is nonplanar, the arrangement of the upper face atoms reflects a palladium {111} facet. Furthermore, the cluster possesses two adjacent face centered cubic (fcc) sites at the top, which are known to be the preferred positions for dissociative hydrogen adsorption.[23]

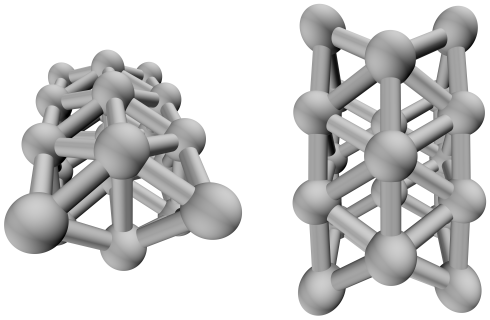


Fig. 2 Structure of the selected Pd_{21} cluster: side view (left) and view from the top (right).

The carbon support materials are modelled by a hydrogen terminated graphene layer. Initial geometries of the palladium clusters were taken from Ahlrichs et al.[48] and Shamsiev et al.[23]. To find the most stable structures of the clusters on the graphene support material, ground-state geometry optimizations starting from different initial orientations have been carried out. The most stable structures of the carbon-supported clusters are shown in Fig. 3 and Fig. 4.

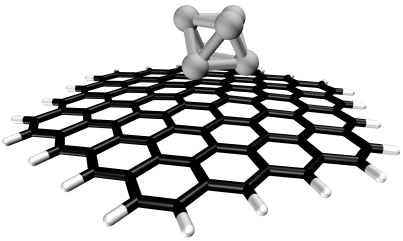


Fig. 3 Most stable structure of the carbon-supported Pd_6 cluster.

The octahedral Pd_6 cluster is oriented such that a palladium triangle is aligned in a parallel fashion to the graphene surface at a distance of about 2.17 Å. The three lower palladium atoms interact each with two carbon atoms (so in total with six carbon atoms) of the support material. In its ground state the carbon-supported Pd_6 cluster has singlet multiplicity.

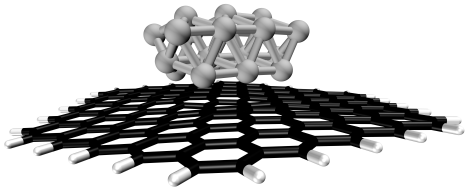


Fig. 4 Most stable structure of the carbon-supported Pd_{21} cluster with {111} facet and fcc sites located at the top of the cluster.

For the Pd_{21} system, the {111} facet as well as the two fcc sites should be located at the top of the carbon-supported cluster, where the hydrogen adsorption process is expected to proceed. In the most stable structure meeting this requirement, the lowest layer of the Pd_{21} cluster is located at around 2.21 Å from the graphene surface. The six palladium atoms of the lowest layer interact in total with 12 carbon atoms (again each palladium interacts with two carbons) of the support material. As the Pd_6 cluster, also the carbon-supported Pd_{21} cluster has singlet multiplicity in its ground state.

To characterize the metal-support interactions and to obtain a measure for the importance of the dispersion contribution, we calculated the binding energy of the systems, once with and once without D3 correction. Even though the D3 correction cannot be identified with the total London dispersion energy, as it only accounts for the long-range part of the latter, it should reproduce for the Pd-support interaction the qualitative trends. Both the Pd_6 and the Pd_{21} system show with binding energies of 195.7 kJ/mol and 549.7 kJ/mol quite strong attractive palladium-carbon-support interactions. The total binding energy increases from the Pd_6 to the Pd_{21} system. The interaction per palladium atom, however, decreases from 32.6 kJ/mol to 26.2 kJ/mol. This fits to the slightly larger cluster-surface-distance in the Pd_{21} system compared to the Pd_6 system. For the Pd_6 system the dispersion contribution of 95.0 kJ/mol makes up around 50 % of the total interaction. For the Pd_{21} system a dispersion contribution of 301.5 kJ/mol was obtained, which corresponds to about 55 % of the total interaction energy. This is in agreement with previous computational studies indicating that the dispersion contribution to metal-support interactions increases with the size of the transition metal cluster.[49] The PBE[45] functional gives slightly lower dispersion contributions for both systems but also shows the trend of higher dispersion contributions for larger clusters (detailed energies can be found in the supporting information†).

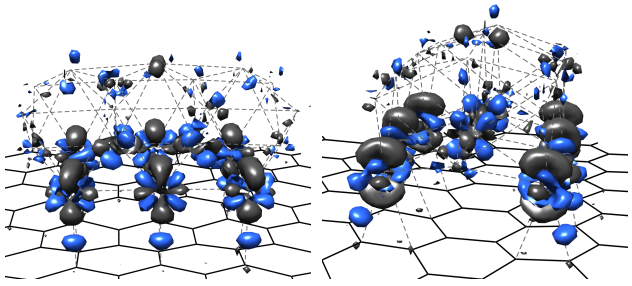


Fig. 5 Change in the electron density induced by the interaction between the Pd_{21} cluster and the support material from two different perspectives. Density gain is colored in blue; density loss is in grey.

The electronic effect of the support material on the Pd clusters is rather small. Therefore, no effect on the Pd−Pd bonding orbitals is noticeable. However, the support material influences the electron density of the clusters. Fig. 5 shows the electron density difference plot for the interaction between the Pd_{21} cluster and the support material. Electron density is shifted from the lowest layer of the Pd cluster into Pd−C connecting lines. This fits to

Physical Chemistry Chemical Physics Accepted Manuscript

View Article Online
DOI: 10.1039/C9CP04606B

Published on 10 September 2019. Downloaded by Ruhr Universitat Bochum on 9/17/2019 4:04:55 PM.

the above conclusion that the interaction of the support material and the Pd cluster is covalent with a strong dispersion contribution. The support has a mostly local effect in the Pd cluster. No charge-transfer into or major changes within the support material are observed. Fig. 6 depicts a Pd−C bonding orbital which has a large Pd d and a smaller C p contribution.

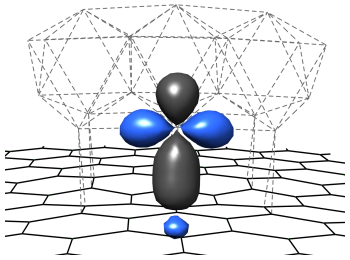


Fig. 6 Visualization of the Pd−C bonding orbital (IBO) for the carbon-supported Pd_{21} cluster.

3.2 Hydrogen adsorption on Pd

As already described in previous studies, e.g. by Lischka *et. al*[16], the adsorption of a hydrogen molecule on a palladium atom leads to an interaction of the empty Pd 5s with the occupied H_2 σ_g orbital and of the occupied Pd $4d_{xz}$ with the empty H_2 σ_u^* orbital (assuming a coordinate system with the x-axis parallel to the H_2 bond and the z-axis parallel to the line from the Pd atom to the H_2 bond center). Fig. 7 shows a visualization of the corresponding IBOs. Furthermore, there is a repulsive interaction between the Pd $4d_{z^2}$ and the H_2 σ_g orbital. As the anti-bonding σ_u^* is populated, the H−H bond is weakened and elongated to 0.93 Å compared to the H−H bond length of 0.76 Å in the isolated H_2 molecule. On the other hand, the Pd−H bond is strengthened.

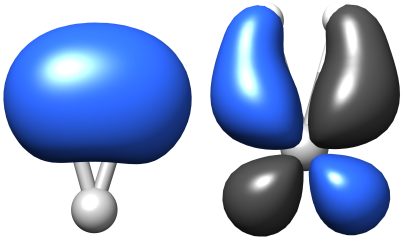


Fig. 7 Visualization of the bonding orbitals (IBOs) of the Pd−H_2 system: 5s-σ_g (left) and $4d_{z^2}$-σ_u^* (right).

Fig. 8 shows the corresponding electron density difference plot. In accordance with the appearance of the bonding orbitals it shows an electron density gain for the 5s Pd and the σ_u^* H_2 orbital and a decreased electron density for the $4d_{xz}$ Pd orbital and the σ_g H_2 orbital.

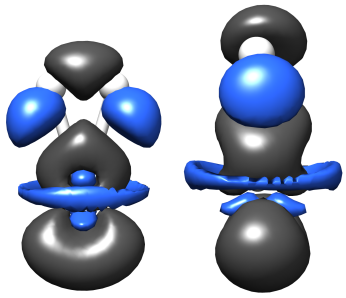


Fig. 8 Electron density difference plot for the Pd−H_2 system from two different perspectives. Density gain is colored in blue; density loss is colored in grey.

3.3 Hydrogen adsorption on Pd_6

The adsorption of H_2 molecules from the gas phase on carbon-supported Pd_6 has been studied and compared to H_2 adsorption on free Pd_6. For both free Pd_6 and carbon-supported Pd_6 molecular hydrogen adsorption can be observed. On free Pd_6 the H_2 molecule adsorbs without a barrier on top of one of the palladium atoms. The adsorption is connected with an energy gain of $\Delta E_{ads} = -49.2$ kJ/mol. In the product (shown in Fig. 9) the H−Pd distance is 1.76 Å. The H−H distance of the H_2 molecule is stretched by around 10 % to 0.85 Å compared to the H−H bond length of 0.76 Å in the gas phase molecule. However, the H−H bond is not broken.

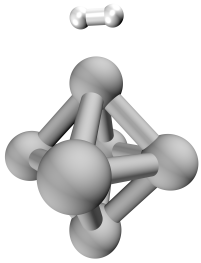


Fig. 9 Product geometry of molecular adsorbed H_2 on free Pd_6.

As mentioned before, results obtained with different functionals and basis sets can differ in the range of some kJ/mol per bond. For a comparison Table 1 shows the hydrogen adsorption energy on the free Pd_6 cluster for the different functionals TPSS[31], BP86[43,44] and PBE[45]. Further exemplary comparisons can be found in the supporting information.†

functional	ΔE_{ads}
TPSS	-49.2
PBE	-63.4
BP86	-61.0

Table 1 Comparison of the hydrogen adsorption energies ΔE_{ads} in kJ/mol on free Pd_6 using three different functionals

On carbon-supported Pd_6 the molecular H_2 adsorption takes preferentially place at one of the palladium atoms located at the top of the cluster. In general, the adsorption process is very similar to the adsorption on the Pd_6 system without carbon support.

Physical Chemistry Chemical Physics Accepted Manuscript

This journal is © The Royal Society of Chemistry [year]

View Article Online
DOI: 10.1039/C9CP04606B

Published on 10 September 2019. Downloaded by Ruhr Universitat Bochum on 9/17/2019 4:04:55 PM.

As for the free Pd_6, the adsorption takes place barrierless and is connected with an energy gain. However, the adsorption energy is with −56.2 kJ/mol on the supported cluster a little bit higher than for the free cluster. The geometry of the product, which is shown in Fig. 10, is very similar to the product geometry without carbon support. A H−Pd distance of 1.78 Å and a H−H distance of 0.84 Å are observed. Only the position of the H_2 molecule with respect to the palladium atom is slightly shifted from a perfect atop position.



Fig. 10 Product geometry of molecular adsorbed H_2 on carbon-supported Pd_6. The carbon support material located below the cluster is not shown.

It is well known that palladium clusters are favourable systems for hydrogen storage. Therefore, it is expected that not only one but several H_2 molecules can adsorb on the Pd_6 clusters. To study this behaviour, we have increased the number of molecular hydrogen adsorbed on the clusters. The incremental adsorption energies ΔE_{ads} and free enthalpies ΔG_{ads} for an increasing number of H_2 molecules are shown for the free and for the carbon-supported Pd_6 clusters in Tables 2 and 3.

number of H_2	ΔE_{ads}	ΔG_{ads}
1	−49.2	−31.3
2	−43.8	−39.3
3	−43.7	−36.8
4	−37.8	−36.5
5	−33.7	−36.5
6	−24.2	−37.2
7	−64.8	−54.0

Table 2 Incremental adsorption energies ΔE_{ads} and Gibbs free enthalpies ΔG_{ads} in kJ/mol for an increasing number of H_2 molecules on free Pd_6

number of H_2	ΔE_{ads}	ΔG_{ads}
1	−56.2	−36.2
2	−33.3	−42.0
3	−33.6	−27.1
4	−66.8	−53.0
4s	−30.5	−47.2

Table 3 Incremental adsorption energies ΔE_{ads} and Gibbs free enthalpies ΔG_{ads} in kJ/mol for an increasing number of H_2 molecules on carbon-supported Pd_6

For the case of the free cluster the seventh H_2 molecule is attached to the same palladium atom as the H_2 molecule number 1. For the carbon-supported Pd_6 the first three H_2 molecules are attached to the palladium atoms at the top of the cluster. The fourth H_2 molecule is either added to a palladium atom at the lower layer of the cluster (4) or alternatively to the same palladium atom as the H_2 molecule number 1 at the top of the cluster (4s). In general, the negative incremental adsorption energies and incremental adsorption free enthalpies in Tables 2 and 3 show that both free and carbon-supported Pd_6 clusters can reach a very high H_2 coverage.

When a second H_2 molecule is added to a palladium atom (e.g. H_2 molecule number 4s for the carbon-supported cluster) the additional H_2 molecule is shared between two palladium atoms (see Fig. 11). If one adds a seventh H_2 molecule to the free Pd_6 cluster, in which all palladium atoms have already been covered with one H_2 molecule, not only one but three H_2 molecules are shared. Thus, each palladium atom can just carry one full H_2 molecule and if the coverage exceeds one H_2 molecule per palladium atom, the H_2 molecules have to be shared. For the carbon-supported Pd_6 cluster the H_2 sharing can also be observed for H_2 molecules, which are added to free palladium atoms of the lower layer of the cluster (e.g. H_2 molecule number 4). Accordingly, the palladium atoms at the lower layer cannot carry one full H_2 molecule. As it would have been expected, the hindrance of the support material reduces the number of H_2 molecules, which can be added to the Pd_6 cluster.

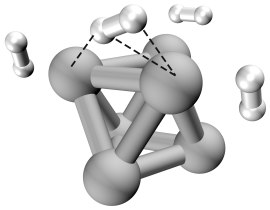


Fig. 11 The fourth H_2 molecule of the 4s geometry of carbon-supported Pd_6 is shared between two palladium atoms. The carbon support material located below the cluster is not shown.

Starting from physisorbed molecular H_2, the molecules can undergo a dissociative chemisorption. A possible reaction pathway for the H_2 dissociation on a carbon-supported Pd_6 cluster is shown in Fig. 12.

As a first step, the H_2 molecule adsorbs at one of the palladium atoms located at the top of the cluster. This is, as described before, related to an energy gain of $\Delta E_{ads} = -56.2$ kJ/mol. Starting from the corresponding minimum of molecular adsorbed hydrogen, the system has to surpass an activation barrier. We have found two different possible transition states, in which one hydrogen atom is bound to one palladium atom and the other hydrogen atom bridges a Pd−Pd bond: a) a transition state from a spin-restricted closed-shell calculation with an energy barrier of 42.0 kJ/mol and a free activation enthalpy of 3.3 kJ/mol showing a cis-configuration of the hydrogen atoms b) an energetically lower lying transition state from a spin-unrestricted calculation with an energy barrier of 21.6 kJ/mol and a free activation enthalpy of 4.1 kJ/mol showing a perpendicular configuration. Starting from the reactants (carbon-supported Pd_6 and a H_2 molecule in the gas phase), the hydrogen dissociation releases an energy of $\Delta E_{diss} = -100.0$ kJ/mol. In the product, the H_2 molecule is fully dissociated; the two hydrogen atoms are sit-

Physical Chemistry Chemical Physics Accepted Manuscript

View Article Online
DOI: 10.1039/C9CP04606B

Published on 10 September 2019. Downloaded by Ruhr Universitat Bochum on 9/17/2019 4:04:55 PM.

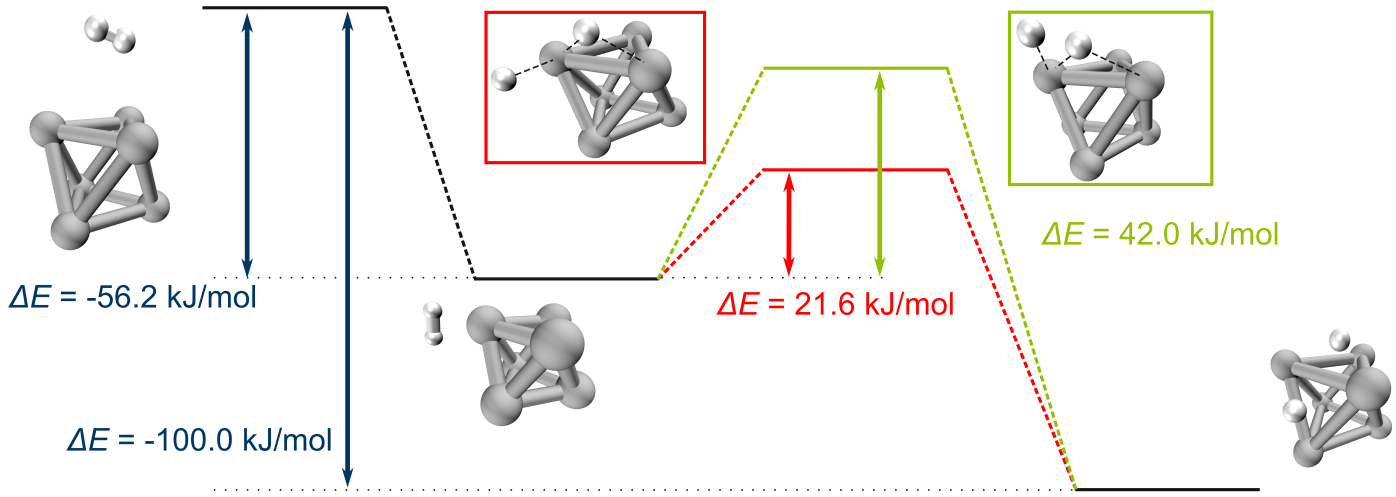


Fig. 12 Possible hydrogen dissociation pathways on carbon-supported Pd_6; in red the result of a spin-unrestricted calculation with a lower energy barrier and in green the result of a spin-restricted closed-shell calculation with a higher barrier. The carbon support material located below the clusters is not shown.

ting on triangular positions each bridging three palladium atoms. The shown reaction pathway and the free activation enthalpies of 3.3 kJ/mol and 4.1 kJ/mol indicate that hydrogen dissociation on a carbon-supported Pd_6 cluster could occur spontaneously at room temperature. The minimal activation energy needed is with 21.6 kJ/mol relatively low and is already provided more than twice by the molecular adsorption process.

As a comparison, Fig. 13 shows the corresponding pathway on free Pd_6. Here, just the energetically lower lying open-shell transition state is included.

In general, the dissociation mechanism on free Pd_6 is very similar to the mechanism on carbon-supported Pd_6. However, the observed energy differences deviate. The adsorption energy ΔE_{ads} and the dissociation energy ΔE_{diss} are with −49.2 kJ/mol and −66.7 kJ/mol smaller than the corresponding energies of −56.2 kJ/mol and −100.0 kJ/mol for the carbon-supported system. The activation energy barrier is with 35.5 kJ/mol by 13.9 kJ/mol higher than for the carbon-supported system. Hence, the carbon support material increases the energy gain of the hydrogen adsorption and dissociation as well as it decreases the activation energy barrier, which has to be surmounted. Therefore, hydrogen adsorption and dissociation are energetically facilitated on carbon-supported Pd_6 clusters compared to free Pd_6. The free activation enthalpy is also for the free system very low (1.4 kJ/mol) and shows that also hydrogen dissociation on free Pd_6 occurs spontaneously at room temperature.

Palladium clusters can support the dissociation of more than one H_2 molecule. We have studied the dissociation of several H_2 molecules one after each other. For the carbon-supported Pd_6 cluster the hydrogen atoms have been added starting from the top of the cluster. The resulting incremental dissociation energies ΔE_{diss} and free enthalpies ΔG_{diss} for an increasing number of H_2 molecules for the free and for the carbon-supported Pd_6 cluster are shown in Tables 4 and 5.

In general, the dissociation energies ΔE_{diss} and dissociation enthalpies ΔG_{diss} in Tables 4 and 5 indicate that a lot of H_2 molecules can be dissociated on the clusters.

number of H_2	ΔE_{diss}	ΔG_{diss}
1	−66.7	−42.4
2	−45.7	−26.7
3	−71.5	−32.5
4	−68.8	−37.6

Table 4 Incremental dissociation energies ΔE_{diss} and Gibbs free enthalpies ΔG_{diss} in kJ/mol for an increasing number of H_2 molecules on free Pd_6

number of H_2	ΔE_{diss}	ΔG_{diss}
1	−100.0	−51.0
2	−62.8	−28.9
3	−106.1	−51.3

Table 5 Incremental dissociation energies ΔE_{diss} and Gibbs free enthalpies ΔG_{diss} in kJ/mol for an increasing number of H_2 molecules on carbon-supported Pd_6

It is important to note that the dissociation of the third H_2 molecule is by an energy of 34.6 kJ/mol and a free enthalpy of 18.8 kJ/mol more favourable on the carbon-supported system compared to the free system, even though the hydrogen atoms have to be added to the unfavourable lower layer of the cluster. The highly favourable ΔE_{diss} and ΔG_{diss} for the third dissociated H_2 molecule on the carbon-supported system can be explained by the fact that adding the two hydrogen atoms of the third H_2 molecules to the lower layer of the cluster leads to a deformation of the cluster (see Fig. 14), which forms a more favourable geometry connected to a favourable dissociation energy and enthalpy. This behaviour can also be observed, if one adds one hydrogen atom of the second H_2 molecule not to the top, but to the unfavourable lower layer of the cluster. During the geometry optimization the cluster deforms and the system still shows a favourable dissociation energy of −64.3 kJ/mol and a favourable

Physical Chemistry Chemical Physics Accepted Manuscript

This journal is © The Royal Society of Chemistry [year]

View Article Online
DOI: 10.1039/C9CP04606B

Published on 10 September 2019. Downloaded by Ruhr Universitat Bochum on 9/17/2019 4:04:55 PM.

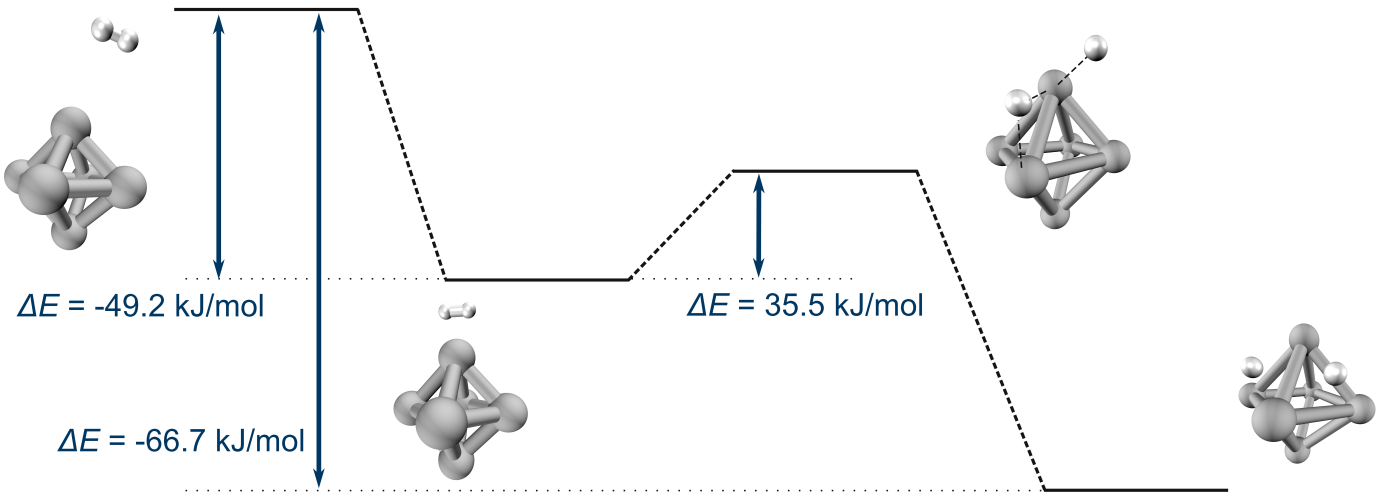


Fig. 13 A possible hydrogen dissociation pathway on free Pd_6.

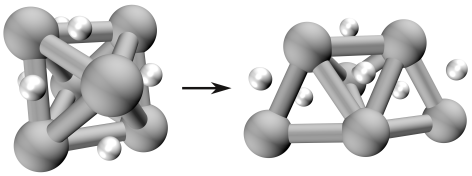


Fig. 14 The geometry of three dissociated hydrogen molecules on carbon-supported Pd_6 before and after geometry optimization. The carbon support material located below the clusters is not shown.

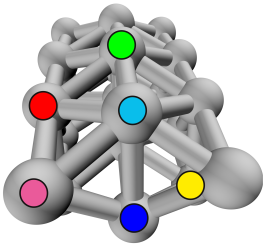


Fig. 15 Studied positions for molecular hydrogen adsorption on Pd_{21}.

dissociation enthalpy of −18.8 kJ/mol.

As such deformations cannot be observed for the free systems, the support material seems to stabilize them. Thus, a high hydrogen coverage on a carbon-supported Pd_6 cluster leads to a deformation of the cluster to a favourable geometry, which is stabilized by the support material. Therefore, the support material allows the cluster for a high hydrogen coverage, in spite of hindrance due to the support material, and facilitates the dissociation of several H_2 molecules compared to free Pd_6.

3.4 Hydrogen adsorption on Pd_{21}

As a model system, which should be closer to real systems under experimental conditions, we studied the adsorption of H_2 molecules from the gas phase on carbon-supported Pd_{21} and compared the results to the H_2 adsorption on free Pd_{21}. On the Pd_{21} systems molecular H_2 adsorption is possible at many different positions with different coordinations. We have studied six different positions for molecular H_2 adsorption, which are shown in Fig. 15. The corresponding adsorption energies ΔE_{ads} for the free and for the carbon-supported Pd_{21} clusters are shown in Tables 6 and 7.

position colored in	ΔE_{ads}
green	−55.9
light blue	−45.6
pink	−40.6
yellow	−34.8
dark blue	−29.9
red	−21.1

Table 6 Adsorption energies ΔE_{ads} in kJ/mol for the different positions studied on free Pd_{21}

position colored in	ΔE_{ads}
green	−45.6
light blue	−42.9
pink	−34.4
yellow	not stable
dark blue	−32.6
red	−30.1

Table 7 Adsorption energies ΔE_{ads} in kJ/mol for the different studied positions on carbon-supported Pd_{21}

For the free Pd_{21} cluster the different H_2 positions are quite similar to each other. The adsorption energies range from −21.1 kJ/mol to −55.9 kJ/mol. In general, the positions at the top of the cluster (green and light blue) are preferred.

The carbon support material reduces the adsorption energies

Physical Chemistry Chemical Physics Accepted Manuscript

View Article Online
DOI: 10.1039/C9CP04606B

Published on 10 September 2019. Downloaded by Ruhr Universitat Bochum on 9/17/2019 4:04:55 PM.

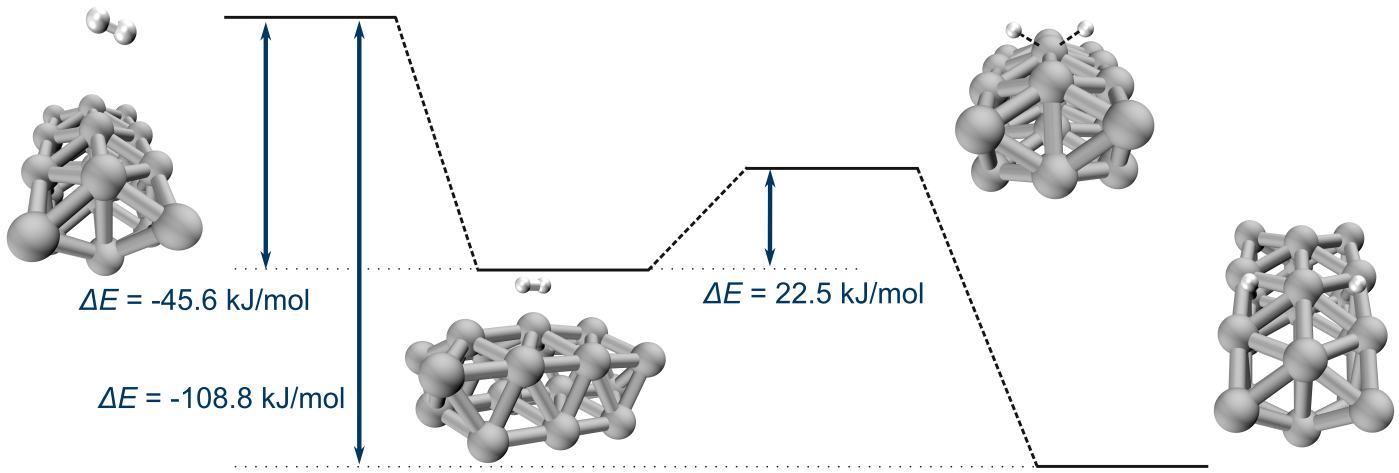


Fig. 16 A possible hydrogen dissociation pathway on carbon-supported Pd_{21}. The carbon support material located below the clusters is not shown.

of the positions colored in green, light blue and pink as well as it increases the corresponding adsorption energies for the dark blue and the red position. The position at the bottom of the cluster (yellow) is not stable, due to steric hindrance by the support material. The adsorption energies for the carbon-supported Pd_{21} cluster range from -30.1 kJ/mol to -45.6 kJ/mol. Accordingly, the most attractive positions for molecular H_2 adsorption on carbon-supported Pd_{21} clusters are by around 10 kJ/mol less favourable than on free Pd_{21}. However, the support material decreases the range of adsorption energies to only 15.5 kJ/mol and therefore levels out the differences between the different positions.

Fig. 17 shows the electron density difference plot for the H_2 molecular adsorption on carbon-supported Pd_{21}. As one would expect, it looks very similar to the electron density difference plot for the H_2 adsorption on a Pd atom. Also here, there is an electron density gain for the 5s Pd and the σ_u^* H_2 orbital and a decreased electron density for the $4d_{xz}$ Pd orbital and the σ_g H_2 orbital. However, it can be observed that, compared to the Pd atom, the Pd cluster allows a partial depopulation of the $4d_{z^2}$ orbital in favour of some other orbitals in the Pd cluster, decreasing the repulsive effect of the $4d_{z^2}$–σ_g interaction.

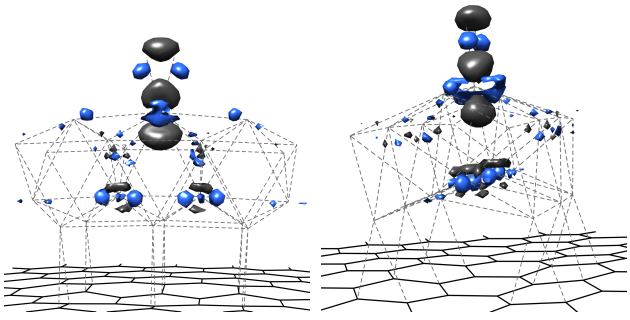


Fig. 17 Electron density difference plot for the H_2 molecular adsorption on carbon-supported Pd_{21} from two different perspectives. Density gain is colored in blue; density loss is colored in grey.

The details of the electronic effect of the carbon support material on the molecular hydrogen adsorption is resolved in Fig. 18 showing the electron density difference plot for the interaction between the carbon support and the most stable Pd_{21}–H_2 system. We observe that the supported system has a higher population of the $4d_{z^2}$ orbital of the Pd atom that adsorbed the H_2. This increases the repulsion between the $4d_{z^2}$ Pd orbital and the σ_g H_2 orbital and, therefore, destabilizes the Pd–H_2 bond and reduces the adsorption energy relative to the unsupported system. The increased adsorption energies for the dark blue and the red H_2 positions are probably due to favorable changes in the geometries. Together these effects reduce the differences between the adsorption energies at the different sites and increase the mobility of the hydrogen on the Pd cluster.

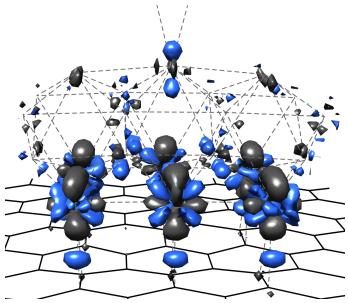


Fig. 18 Electron density difference plot for the interaction between the carbon support and the most stable Pd_{21}–H_2 system. Density gain is colored in blue; density loss is colored in grey.

Also on Pd_{21} molecular adsorbed H_2 can undergo dissociative chemisorption. A possible reaction pathway for the H_2 dissociation on a carbon-supported Pd_{21} cluster is shown in Fig. 16. In a first step the H_2 adsorbs as a molecule at the most favourable site (green position in Fig. 15) releasing an energy of $\Delta E_{ads} = -45.6$ kJ/mol. Starting from this minimum, the systems goes through a transition state with an energy barrier of 22.5 kJ/mol and then builds the product of fully dissociated hydrogen, in which the two hydrogen atoms are located at the adjacent fcc

Physical Chemistry Chemical Physics Accepted Manuscript

This journal is © The Royal Society of Chemistry [year]

View Article Online
DOI: 10.1039/C9CP04606B

Published on 10 September 2019. Downloaded by Ruhr Universitat Bochum on 9/17/2019 4:04:55 PM.

sites. The overall dissociation energy ΔE_{diss} is −108.8 kJ/mol. The corresponding pathway on free Pd_{21} looks very much the same. However, the reaction energies are slightly different. As mentioned above, the adsorption energy of H_2 at the most favourable position is with −55.9 kJ/mol higher for the free than for the carbon-supported cluster. Also the dissociation energy is with −127.9 kJ/mol higher on the free cluster. In contrast to this, the activation energy barrier is slightly reduced to 11.3 kJ/mol which corresponds to a free activation enthalpy of 2.7 kJ/mol. Close to the transition state the potential energy surface of the system is very flat. Thus, a full transition state optimization was not possible and the vibrational analysis of the transition state described here still shows three negative eigenvalues. However, we expect the errors introduced by this to be negligible. For the calculation of the free activation enthalpy, the additional negative eigenvalues have not been included in the zero-point vibrational energy.

It is important to note that the hydrogen dissociation pathways on carbon-supported Pd_6 and carbon-supported Pd_{21} are very similar to each other. Even the observed adsorption and dissociation energies and activation barriers agree very well. Also hydrogen dissociation on a carbon-supported Pd_{21} cluster can occur spontaneously at room temperature.

On the Pd_{21} clusters the H_2 molecule has different possibilities to dissociate. We have studied six different configurations for the two hydrogen atoms, which are shown in Fig. 19. The corresponding dissociation energies ΔE_{diss} for the free and for the carbon-supported Pd_{21} clusters are listed in Tables 8 and 9.

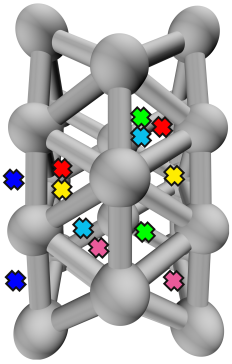


Fig. 19 Studied configurations for dissociated hydrogen on Pd_{21}.

positions colored in	ΔE_{diss}
yellow	−127.9
red	−124.6
light blue	−109.1
green	−107.6
pink	−102.4
dark blue	−88.7

Table 8 Dissociation energies ΔE_{diss} in kJ/mol for the different studied positions on free Pd_{21}

For the free Pd_{21} cluster the different configurations of the two hydrogen atoms are quite similar to each other. The dissociation energies ΔE_{diss} range from −88.7 kJ/mol to −127.9 kJ/mol. In general, the positions at the top of the cluster (yellow, red, light blue and green) are preferred over configurations in which one (pink) or both (dark blue) hydrogen atoms are located at the side of the cluster. In the most favourable configuration (yellow) the two hydrogen atoms are located at the adjacent fcc sites. The effect of the carbon support material on the dissociation energies is quite similar to its effect on the H_2 adsorption energies. The dissociation energy for the most favourable configurations is decreased by around 20 kJ/mol compared to the free Pd_{21} system. The range of dissociation energies is reduced to only 15.3 kJ/mol. As a conclusion, the carbon support material also levels out the differences between different configurations of the hydrogen atoms after H_2 dissociation.

positions colored in	ΔE_{diss}
yellow	−108.8
red	−98.5
light blue	−93.5
green	−93.6
pink	−101.5
dark blue	−95.0

Table 9 Dissociation energies ΔE_{diss} in kJ/mol for the different studied positions on carbon-supported Pd_{21}

The electron density difference plot for the influence of the carbon support material on the hydrogen dissociation on Pd_{21} does not show any relevant shifts in the electron density. However, the H_2 dissociation on both free and carbon-supported Pd_{21} is connected to quite a strong change of geometry around the hydrogen atoms. Fig. 20 shows a sketch of the six relevant Pd−Pd distances for the free and the carbon-supported system each with and without dissociated H_2 in the fcc positions.

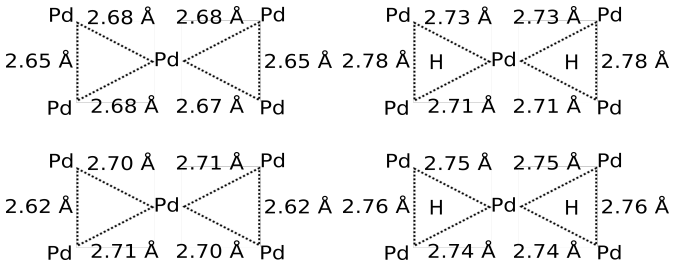


Fig. 20 Sketch of the six relevant Pd−Pd distances for the free (top) and the carbon-supported (bottom) system each with (right) and without (left) dissociated H_2 in the fcc positions.

If the hydrogen atoms are added to the free cluster, the Pd−Pd bonds are elongated. The largest change can be observed at the edge of the cluster, where the bond is elongated by 0.13 Å from 2.65 to 2.78 Å. The Pd−Pd distances at the top of the cluster show changes between 0.03 Å and 0.05 Å. For the carbon-supported cluster a very similar behavior can be observed. There, the Pd−Pd bonds are elongated by 0.14 Å at the edge of the cluster and from 0.03 Å to 0.05 Å at the top of the cluster. In general, the distances on the free and on the carbon-supported clusters are nearly the same, both with and without dissociated H_2. However, the sup-

Physical Chemistry Chemical Physics Accepted Manuscript

View Article Online
DOI: 10.1039/C9CP04606B

Published on 10 September 2019. Downloaded by Ruhr Universitat Bochum on 9/17/2019 4:04:55 PM.

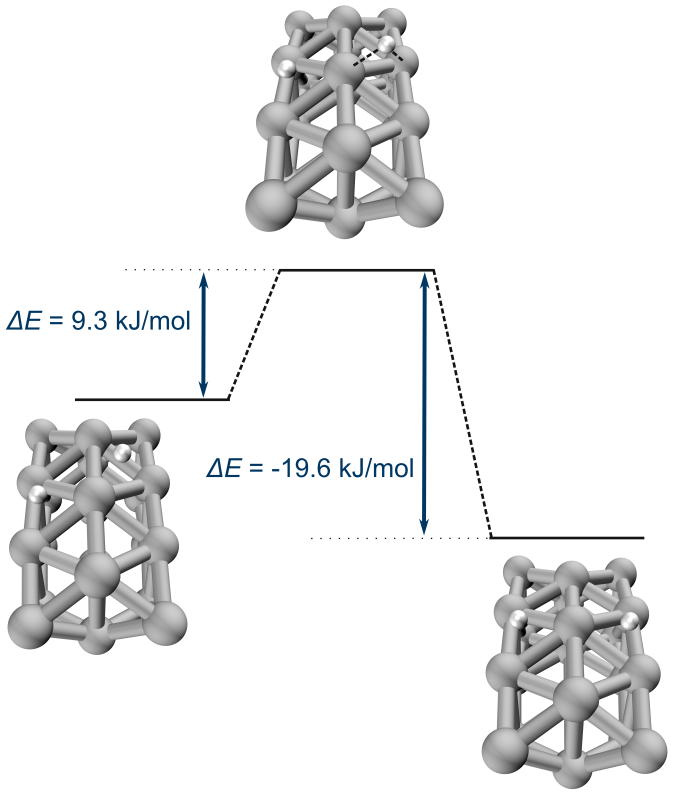


Fig. 21 Hydrogen migration pathway from the red to the yellow configuration on carbon-supported Pd_{21}. The carbon support material located below the clusters is not shown.

port material hinders the relaxation of the rest of the system after the Pd−Pd bond elongation and, as can be seen in the geometry, leads to a deformation of the support material. This explains the decreased H_2 dissociation energy for the carbon-supported cluster. The increased H_2 dissociation energy for the pink and the dark blue systems is probably due to geometrical changes in the H_2 positions.

The hydrogen atoms can migrate between the different positions on the cluster. A possible migration pathway between the yellow and the red configuration on carbon-supported Pd_{21} is shown in Fig. 21. The transition state, in which one hydrogen atom bridges a Pd−Pd bond, has an activation energy barrier of 9.3 kJ/mol starting from the less favourable red configuration and an activation energy barrier of 19.6 kJ/mol starting from the most favourable yellow configuration. Accordingly, hydrogen atom migration on carbon-supported Pd_{21} could occur spontaneously at room temperature, especially when the hydrogen atoms are not located in the most stable configuration.

The migration pathway on free Pd_{21} looks exactly the same as the pathway on carbon-supported Pd_{21} in Fig. 21. The activation energy barrier for the migration from the less favourable red configuration is with 8.3 kJ/mol very similar to the corresponding activation barrier for the carbon-supported system. However, the activation energy barrier for the migration starting from the yellow configuration is only 11.6 kJ/mol.

The free activation enthalpies are 10.5 kJ/mol for the migration from the red configuration and 6.3 kJ/mol for the migration from the yellow configuration. This confirms the conclusion drawn from the activation energies that hydrogen migration on Pd_{21} clusters should occur spontaneously at room temperature.

4 Conclusions

The present study provided an in-depth inside into metal-support interactions for carbon-supported palladium clusters and their influence on hydrogen adsorption. Palladium clusters show quite strong attractive palladium-carbon interactions. The dispersion contribution to the interaction increases with the system size. The support material has a rather small and local effect on the electronic structure. No changes in bonding orbitals can be observed. The metal-support interaction is based on a shift of electron density from the lowest layer of the cluster to the support-metal connecting line, indicating directed partially covalent Pd−C interactions.

In general, hydrogen adsorption on palladium clusters would at low temperatures proceed stepwise. First, the H_2 molecule is physisorbed. In a second step, the H_2 molecule undergoes dissociative chemisorption. The corresponding reaction pathways for the systems with and without carbon support are very similar to each other. However, the carbon support material has an effect on the observed energies. For the case of Pd_6 the carbon support increases the adsorption and dissociation energy and lowers the activation energy barrier. For the Pd_{21} systems the effect of the carbon support material depends on the position. All in all, the support decreases adsorption energies at the top site by hindering the depopulation of the $4d_{z^2}$ orbital and also decreases the dissociation energies at these sites by geometrical constrains. However, a destabilization of the quite attractive palladium-hydrogen interaction might be in favour of catalytic activity as it increases the mobility of the hydrogen on the cluster. Furthermore, the support material reduces the differences between different positions and facilitates the H_2 adsorption and dissociation at different positions on the cluster. The free activation enthalpies show that at room temperature H_2 dissociation should occur spontaneously both on free and on carbon-supported palladium clusters.

With and without carbon support material palladium clusters can adsorb several hydrogen molecules. If one adds more than one H_2 molecule per palladium atom the palladium atoms start to share hydrogen molecules. For the carbon-supported systems the hindrance of the support material reduces the number of H_2 molecules, which can be added to the cluster. Dissociation of several hydrogen molecules on free and on carbon-supported palladium clusters is energetically favourable and shows negative reaction enthalpies at room temperature. The carbon support material facilitates the dissociation of several hydrogen molecules on the clusters, especially by stabilizing geometrical deformations. Hydrogen atom migration can occur spontaneously at room temperature on free and on carbon-supported palladium clusters.

In general, the Pd_6 and Pd_{21} systems show very similar pathways and energies. Accordingly, already the quite small carbon-supported Pd_6 clusters are good model systems for reaction pathways. However, Pd_6 cannot model special properties of palladium nanoparticles. So it does not show the decrease in adsorption

Physical Chemistry Chemical Physics Accepted Manuscript

This journal is © The Royal Society of Chemistry [year]

View Article Online
DOI: 10.1039/C9CP04606B

Published on 10 September 2019. Downloaded by Ruhr Universitat Bochum on 9/17/2019 4:04:55 PM.

and dissociation energies caused by the carbon support material, which might increase the catalytic activity of the palladium cluster. Furthermore, the hydrogen atom migration or the differences between different adsorption sites, which will definitely affect the hydrogenation process in experiments, cannot be studied on Pd_6. Therefore it is essential to also take larger cluster sizes as Pd_{21} into account.

The present study on hydrogen adsorption helps to achieve a deeper understanding of hydrogenation reactions employing mesoporous carbon as the support material and will be a good starting point for subsequent studies focusing on the effect of nitrogen or oxygen doping on the hydrogenations. For instance, in experiments it can be observed that hydrogen atoms, which are attached to a carbon-supported metal-nanoparticle, can migrate from the metal to the support material. This so called hydrogen spillover especially occurs on nitrogen-doped carbon support materials and might play an important role in hydrogenation reactions.[50] The low energy barriers and low free activation enthalpies for hydrogen atom migration on Pd_{21} clusters obtained in the present study give some evidence that hydrogen spillover might actually be possible. We plan to investigate the hydrogen spillover in more detail in a subsequent study.

Conflicts of interest

There are no conflicts to declare.

Acknowledgements

This work has been supported by the Deutsche Forschungsgemeinschaft and the National Natural Science Foundation of China within the framework of the Sino-German initiative "Novel Functional Materials for Sustainable Chemistry" through grant Ha 2588/9-1.

References

1 W. Ludwig, A. Savara, K.-H. Dostert and S. Schauermann, *J. Catal.*, 2011, **284**, 148–156.
2 F. Zaera, *ACS Catal.*, 2017, **7**, 4947–4967.
3 A. Stanislaus and B. H. Cooper, *Catal. Rev.: Sci. Eng.*, 1994, **36**, 75–123.
4 *Catalytic Hydrogenation*, ed. L. Cervený, Elsevier Science, 1986, vol. 27.
5 V. Kratky, M. Kralik, M. Mecarova, M. Stolcova, L. Zalibera and M. Hronec, *Appl. Catal., A*, 2002, **235**, 225–231.
6 D. M. Alonso, J. Q. Bond and J. A. Dumesic, *Green Chem.*, 2010, **12**, 1493–1513.
7 A. T. Bell, *Science*, 2003, **299**, 1688–1691.
8 N. M. Julkapli and S. Bagheri, *Int. J. Hydrogen Energy*, 2015, **40**, 948–979.
9 T. E. Felter, E. C. Sowa and M. A. Van Hove, *Phys. Rev. B*, 1989, **40**, 891–899.
10 K. Christmann, *Surf. Sci. Rep.*, 1988, **9**, 1–163.
11 M. Johansson, E. Skúlason, G. Nielsen, S. Murphy, R. Nielsen and I. Chorkendorff, *Surf. Sci.*, 2010, **604**, 718–729.
12 A. Tomaszewska, A. Ciszewski and Z. M. Stępień, *Appl. Surf. Sci.*, 2008, **254**, 4386–4390.
13 T. Mitsui, M. Rose, E. Fomin, D. Ogletree and M. Salmeron, *Surf. Sci.*, 2003, **540**, 5–11.
14 J.-F. Paul and P. Sautet, *Phys. Rev. B*, 1996, **53**, 8015–8027.
15 V. Ledentu, W. Dong and P. Sautet, *Surf. Sci.*, 1998, **412-413**, 518–526.
16 M. Lischka and A. Groß, *Phys. Rev. B*, 2002, **65**, 075420.
17 Y. Zhao and D. Tian, *Comput. Theor. Chem.*, 2012, **991**, 40–43.
18 J. Moc, D. G. Musaev and K. Morokuma, *J. Phys. Chem. A*, 2000, **104**, 11606–11614.
19 J. Moc, D. G. Musaev and K. Morokuma, *J. Phys. Chem. A*, 2003, **107**, 4929–4939.
20 Y. Wang, Z. Cao and Q. Zhang, *Chem. Phys. Lett.*, 2003, **376**, 96–102.
21 C. Zhou, S. Yao, J. Wu, R. C. Forrey, L. Chen, A. Tachibana and H. Cheng, *Phys. Chem. Chem. Phys.*, 2008, **10**, 5445–5451.
22 A. W. Pelzer, J. Jellinek and K. A. Jackson, *J. Phys. Chem. A*, 2015, **119**, 3594–3603.
23 R. S. Shamsiev and F. O. Danilov, *Russ. Chem. Bull.*, 2017, **66**, 395–400.
24 A. Granja-DelRío, J. A. Alonso and M. J. López, *Comput. Theor. Chem.*, 2017, **1107**, 23–29.
25 I. López-Corral, E. Germán, A. Juan, M. A. Volpe and G. P. Brizuela, *J. Phys. Chem. C*, 2011, **115**, 4315–4323.
26 C. Ramos-Castillo, J. Reveles, R. Zope and R. de Coss, *J. Phys. Chem. C*, 2015, **119**, 8402–8409.
27 A. Lu, A. Kiefer, W. Schmidt and F. Schüth, *Chem. Mater.*, 2004, **16**, 100–103.
28 Y. Huang, F. Yang, Z. Xu and J. Shen, *J. Colloid Interface Sci.*, 2011, **363**, 193–198.
29 J. Cai, S. Bennici, J. Shen and A. Auroux, *Microporous and Mesoporous Mater.*, 2015, **212**, 156–168.
30 J. Tao, J. P. Perdew, V. N. Staroverov and G. E. Scuseria, *Phys. Rev. Lett.*, 2003, **91**, 146401.
31 F. Weigend and R. Ahlrichs, *Phys. Chem. Chem. Phys.*, 2005, **7**, 3297–3305.
32 D. Andrae, U. Häußermann, M. Dolg, H. Stoll and H. Preuß, *Theor. Chim. Acta*, 1990, **77**, 123–141.
33 F. Furche and J. P. Perdew, *The Journal of Chemical Physics*, 2006, **124**, 044103.
34 D. Stodt, H. Noei, C. Hättig and Y. Wang, *Phys. Chem. Chem. Phys.*, 2013, **15**, 466–472.
35 J. Koßmann and C. Hättig, *Phys. Chem. Chem. Phys.*, 2012, **14**, 16392–16399.
36 *TURBOMOLE V7.1 2016, V7.2.1 2017 and V7.3 2018, a development of University of Karlsruhe and Forschungszentrum Karlsruhe GmbH, 1989-2007, TURBOMOLE GmbH, since 2007; available from* `http://www.turbomole.com`.
37 M. Sierka, A. Hogekamp and R. Ahlrichs, *J. Chem. Phys.*, 2003, **118**, 9136–9148.
38 F. Weigend, *Phys. Chem. Chem. Phys.*, 2006, **8**, 1057–1065.
39 S. Grimme, J. Antony, S. Ehrlich and H. Krieg, *J. Chem. Phys.*, 2010, **132**, 154104.
40 P. Plessow, *J. Chem. Theory Comput.*, 2013, **9**, 1305–1310.

Physical Chemistry Chemical Physics Accepted Manuscript

View Article Online
DOI: 10.1039/C9CP04606B

41 T. Helgaker, *Chem. Phys. Lett.*, 1991, **182**, 503–510.
42 K. Fukui, *Acc. Chem. Res.*, 1981, **14**, 363–368.
43 A. D. Becke, *Phys. Rev. A*, 1988, **38**, 3098–3100.
44 J. P. Perdew, *Phys. Rev. B*, 1986, **33**, 8822–8824.
45 J. P. Perdew, K. Burke and M. Ernzerhof, *Phys. Rev. Lett.*, 1996, **77**, 3865–3868.
46 G. Knizia, *J. Chem. Theory Comput.*, 2013, **9**, 4834–4843.
47 K. A. Peterson, D. Figgen, M. Dolg and H. Stoll, *J. Chem. Phys.*, 2007, **126**, 124101.
48 P. Nava, M. Sierka and R. Ahlrichs, *Phys. Chem. Chem. Phys.*, 2003, **5**, 3372–3381.
49 W. B. Schneider, U. Benedikt and A. A. Auer, *ChemPhysChem*, 2013, **14**, 2984–2989.
50 W. C. Conner and J. L. Falconer, *Chem. Rev.*, 1995, **95**, 759–788.

Published on 10 September 2019. Downloaded by Ruhr Universitat Bochum on 9/17/2019 4:04:55 PM.

Physical Chemistry Chemical Physics Accepted Manuscript

This journal is © The Royal Society of Chemistry [year]